Accelerated mechanochemical bond scission and stabilization against heat and light in carbamoyloxime mechanophores

Simay Aydonat,[1,2,3,7] Davide Campagna,[2,3,7] Sourabh Kumar,[4] Sonja Storch,[2,3] Tim Neudecker,[4,5,6]* and Robert Göstl[1,2,3,8]*

[1]Department of Chemistry and Biology, University of Wuppertal, Wuppertal, Germany

[2]DWI – Leibniz Institute for Interactive Materials, Aachen, Germany

[3]Institute of Technical and Macromolecular Chemistry, RWTH Aachen University, Aachen, Germany

[4]Institute for Physical and Theoretical Chemistry, University of Bremen, Bremen, Germany

[5]Bremen Center for Computational Materials Science, Bremen, Germany

[6]MAPEX Center for Materials and Processes, Bremen, Germany

[7]These authors contributed equally

[8]Lead contact

*Correspondence: neudecker@uni-bremen.de, goestl@uni-wuppertal.de

Summary

Current approaches to the discovery of mechanochemical reactions in polymers are limited by the interconnection of the zero-force and force-modified potential energy surfaces, since most mechanochemical reactions are force-biased thermal reactions. Here, carbamoyloximes are developed as a mechanophore class in which the mechanochemical reaction rates counterintuitively increase together with the thermal stability. All carbamoyloxime mechanophores undergo force-induced homolytic bond scission at the N–O bond and their mechanochemical scission rate increases with the degree of substitution on the α-substituent. Yet, carbamoylaldoximes react to both heat and light with a pericyclic *syn* elimination while carbamoylketoximes undergo thermal decomposition at high temperature and photochemical homolytic scission only from the triplet state. Thereby, the mechanochemical and thermal reaction trajectories are separated and the thermal stability increases

alongside the mechanochemical reaction kinetics. This approach may play an important role in the future of systematic mechanochemical reaction discovery.

Keywords

mechanochemistry, mechanophores, photochemistry, polymers

Introduction

The application of extensional strain to a polymer ultimately leads to random covalent backbone scission in the chain segment with the highest mechanical force concentration.[1] The selectivity of this process can be increased by the incorporation of mechanochemically reactive predetermined breaking points, so-called mechanophores,[2,3] as well as by the choice of polymer architecture.[4,5] The conception of mechanophores has led to exciting applications, for example in force sensing[6–13] and force-activated chemical reactivity.[14–20] Fundamentally, a mechanophore must have a smaller ultimate strength than the macromolecular backbone in the material under investigation. Engineering of its mechanochemical reactivity is hence necessary, but not straightforward, since intuitive molecular design guidelines for mechanochemistry are underdeveloped.[21] Since mechanochemical reactions are force-biased thermal reactions,[22] the mechanochemical and thermal reactivity are generally interconnected. Several examples have been reported where the mechanochemical reaction has been shown to proceed through an alternative, pseudopericyclic, and Woodward-Hoffmann-forbidden pathway and leads to reactivities or product distributions that are unobtainable by the concurrent thermal reaction.[23–31] Yet, for non-pericyclic mechanochemical reactions the dilemma remains where mechanophores are conceived by making them thermally labile. This hampers their successful application due to an accordingly restrictive processing parameter space.[32,33] In a notable example, Otsuka and coworkers have reported the thermal stabilization under retention of the mechanophore character.[34] However, a concomitant increase of scission rate and thermal stability at the same time has never been achieved.

Recently, we have reported carbamoyloximes as a new mechanophore class to protect latent amines.[35] We have shown that carbamoylaldoximes undergo force-induced homolytic bond scission at the N−O

oxime bond where one chain fragment radical decarboxylates to yield the free amine and the other forms a nitrile (**Figure 1**, AO pathway). We hypothesize that the introduction of alkyl substituents R in the α-position of the oxime moiety may affect its mechanochemical reactivity twofold: (i) steric perturbation and elongation of the oxime bond and (ii) electronic stabilization of the mechanochemically formed iminyl radical by hyperconjugation.[36] We speculate that both effects will increase the mechanochemical reactivity of the carbamoyloxime motif by lowering the necessary activation energy E_a.

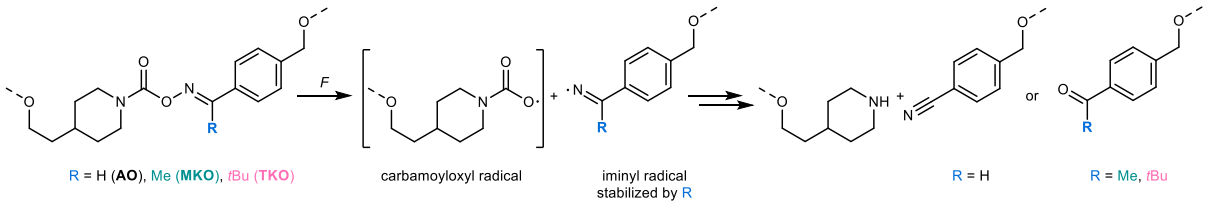

Figure 1. Force-induced homolytic scission of carbamoyloximes at the N–O bond. The product distribution as well as thermal, photochemical, and mechanochemical reactivity depend on the α-substituent R. Dashed bonds indicate connection points to the polymer architecture.

Here we show that these carbamoylketoximes undergo force-induced N–O scission just as carbamoylaldoximes, but afford a final ketone due a different radical pathway (**Figure 1**, **MKO** and **TKO** pathways). We demonstrate that carbamoylketoximes show increased mechanochemical reaction rates compared to their aldoxime counterparts and that this rate increase correlates with the degree of substitution on the α-substituent R. Surprisingly, we find that the thermal and photochemical stabilities of carbamoyloximes increase as well with the introduction of the α-substituent, suggesting diverging reaction trajectories on the zero-force and on the force-modified potential energy surface, which we uncover using combined experimental and computational techniques. Thereby, we present a counterintuitive example of a non-pericyclic mechanophore class where both mechanochemical reaction rate and thermal stability increase together, which may serve as a mechanistic example for future systematic mechanophore discoveries.

Results and discussion

Syntheses of mechanophores and polymers

The carbamoyloxime mechanophores were prepared following an adapted protocol established by us before[35] and the synthesis is detailed in the Supplemental Information (**Figure S1**). Briefly, a carbamoylimidazolinium salt was reacted with the corresponding oximes to obtain the diol precursors of the aldoxime (**AO**, R = H), the methylketoxime (**MKO**, R = Me), and the *t*-butylketoxime (**TKO**, R = *t*Bu). Importantly, all carbamoyloximes showed well-distinguishable ^{1}H NMR spectra (**Figure S16**, **S22**, and **S36**) facilitating the observation of their reaction conversions. Subsequently, the diols were incorporated into the center of linear poly(methyl acrylate) (PMA) chains by esterification to the bifunctional initiator and subsequent telechelic Cu^{0}-mediated controlled radical polymerization yielding the corresponding polymers **PAO**, **PMKO**, and **PTKO** each in five different molar masses M_n (**Table S1**).

Mechanochemical reactivities

Initially, density functional theory (DFT)[37,38] computations using the COnstrained Geometries simulate External Force (COGEF)[39,40] method at the B3LYP/6-31G(d) level of theory,[41–44] followed by calculations of the restoring force at the geometries immediately before dissociation of the molecule, were performed to evaluate the mechanochemical reactivity of the carbamoyloximes (**Figure 2A**). We found that an increasing degree of substitution on R led to a decreasing scission force with (typically by COGEF overestimated)[45] F_{max} of 5.55 nN, 5.22 nN, and 4.55 nN in THF on respectively truncated versions of **AO**, **MKO**, and **TKO** (**Figure S4A**, **Table S22**), qualitatively underlining our initial hypothesis. Variation of the solvent did not show notable qualitative deviations from this trend (**Table S22**).

The mechanochemical selectivity of **PAO** was determined by us before to 42-66%, depending on the sonication conditions and M_n.[35] We hence ultrasonicated **PMKO** with M_n = 103 kDa (**PMKO$_{103}$**) in solution using an immersion probe sonicator at 20 kHz (**Figure 2B**).[46] Variations in solvent, amplitude, and mass concentration (**Table S3**) consistently confirmed the mechanochemical generation of the ketone with selectivities of 44 to 57%, which was verified by the dedicated synthesis of a PMA-

substituted ketone control compound. Identical experiments for **PTKO$_{92}$** yielded selectivities of 46 to 57% (**Table S3**). Polar solvents, and in particular H_2O, equally accelerated the mechanochemical bond scission for all carbamoyloximes, as would be expected due to stronger inertial cavitation.[35,46] The product distributions and mechanochemical selectivities remained largely unaffected.[35]

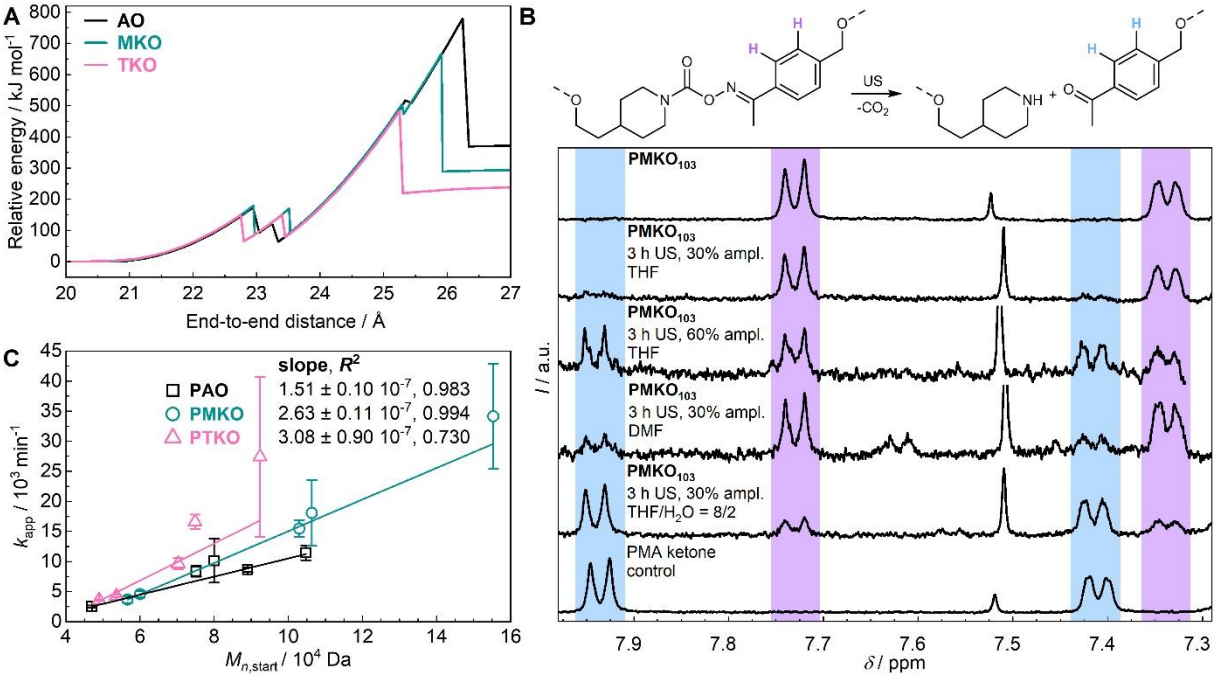

Figure 2. Mechanochemical scission of the carbamoyloxime mechanophores. (A) COGEF computations showing relative energy increase upon stretching of **AO**, **MKO**, and **TKO** in the gas phase. **(B)** Reaction scheme and ^{1}H NMR in $CDCl_3$ excerpts of the mechanochemical **PMKO$_{103}$** scission upon ultrasonication under varying amplitudes and solvents (**Table S2** and **S3**, entries 1-4) including a PMA-appended ketone control compound **23**. **(C)** Comparative plot of the rate constants (calculated according to the initial rates method)[47] against the starting molar mass $M_{n,start}$ for every sonicated sample of **PAO**, **PMKO**, and **PTKO**. Mean values ± SD from the mean. $N = 2$ independent sonications.

The apparent mechanochemical scission rate constants k_{app} were then measured by sonicating the three carbamoyloxime derivative polymers at five different M_n each in duplicate in dilute THF solutions using pulsed ultrasonication (1 s on, 1 s off, 2 to 8 °C, 30% amplitude, power intensity $I_P = 7.4$ W·cm^{-2}, **Table S1** and **S4**). Gel permeation chromatography (GPC) measurements before and after each sonication allowed to plot k_{app} against the initial molar mass $M_{n,start}$ (**Figure 2C** and **Table S4,5**). k_{app} were determined from the time-dependent attenuation of the GPC refractive index (RI) signal corresponding to the initial polymer peak using the initial rates method.[47,48] This method was selected since the respective product formation was minimally affected by competing pathways (*e.g.*, non-selective or secondary scission) in the early stages of ultrasonication. These experiments unambiguously established

the mechanophore character of the carbamoylketoximes and proved the reactivity trend **TKO**>**MKO**>**AO** predicted by COGEF simulations.

Thermal stabilities

Subsequently, the thermal stabilities of the carbamoyloximes were investigated on the small molecule diols at 90, 130, and 170 °C each for 24 h in DMSO-d_6 after which DMF was added as internal standard for NMR measurements (**Table S21**). At 90 °C, **AO** was quantitatively converted to its corresponding nitrile confirming previous observations (**Figure 3A**).[35] **MKO** and **TKO** showed considerably higher thermal stabilities and ketone formation was not observed.[49] Both **MKO** and **TKO** were stable at 130 °C and converted into an unidentifiable mixture of decomposition products at 170 °C (**Figure 3B** and **C**).

An in-depth kinetic analysis of the thermal conversion was conducted by Variable Temperature (VT) NMR measurements obtaining the reactant concentrations through the integrals of the diagnostic peaks in combination with DMF as internal standard. For **AO** conversion, both **AO** consumption and nitrile formation expectedly followed first-order kinetics (**Figure S3A**, **B**, and **C**). Rate constants were extracted at 90, 95, and 100 °C giving E_a = 132 kJ mol^{-1} using Arrhenius fitting (**Figure S3D**). Since **MKO** and **TKO** were thermally stable and degraded non-specifically, their thermal E_a could not be determined. Carbamoylketoximes derived from secondary amines are not prone to thermally dynamic behavior, and hence this mechanistic interpretation was disregarded as an explanation.[50,51] Considering the contrasting mechanochemical reactivity of the carbamoyloximes, these substantial deviations were thus surprising and suggested that the homolytic mechanochemical reaction pathway deviated from the thermal reaction pathway for **AO**.

To understand this behavior, we used DFT at the B3LYP/6-31G(d) level to calculate the zero-force E_a for the homolytic dissociation of the carbamoyloxime mechanophores along the N–O bond in different solvents (**Table S23**). For the thermal dissociation in DMF, 139, 230, and 214 kJ mol^{-1} were found for **AO**, **MKO**, and **TKO**. This trend was essentially also solvent-independent and reflected the experimentally determined thermal stabilities – particularly comparing E_a of **AO** scission with 139 kJ mol^{-1} determined by DFT and 132 kJ mol^{-1} obtained experimentally. Overall, both experiment

and computation suggested a counterintuitive increasing mechanochemical reaction rate with simultaneous increasing thermal stability.

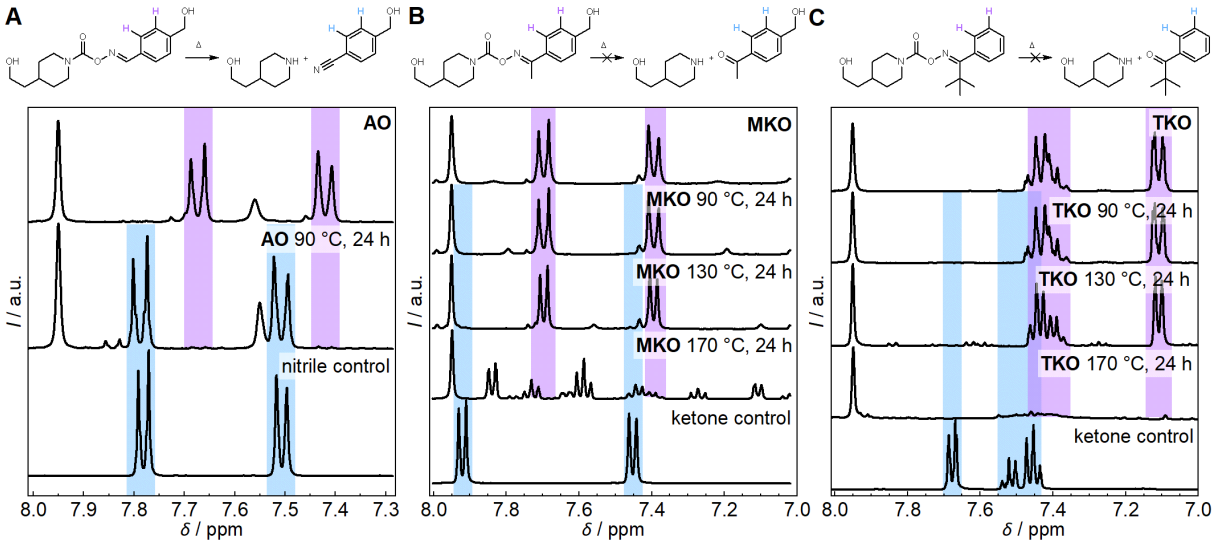

Figure 3. Thermal reactivities of the carbamoyloxime mechanophores. Reaction schemes and ^{1}H NMR in DMSO-d_6 excerpts of the thermal small molecular carbamoylaldoxime degradation at different temperatures including the commercial nitrile and ketone control compounds of **(A) AO**, **(B) MKO**, and **(C)** a **TKO** control compound. Every reaction entry is indicated in **Table S21**.

Investigation of the reaction mechanisms

To unravel the origin of the observed effects, the dissociation mechanism of the carbamoyloxime mechanophores was investigated with a series of intermediate trapping experiments (**Figure 4A**). First, **AO** was heated to its dissociation temperature at 90 °C for 1 h in the presence of the spin trap 5,5-dimethyl-1-pyrroline-*N*-oxide (DMPO) to scavenge and label any radical intermediates.[52] Over the course of the experiment, the nitrile formed expectedly but the DMPO concentration remained constant and no indicative shifts in the ^{1}H NMR spectrum were discerned that hinted towards its reaction with a radical intermediate (**Figure 4B**, **Figure S8**). In a parallel experiment, the photochemical **AO** scission was investigated by irradiation of **AO** at 254 nm for 1 h in the presence of DMPO, which also cleanly produced the nitrile but did not reveal any trapped radicals.

With the indication that both thermal and photochemical **AO** scission might be non-homolytic, we revisited zero-force DFT calculations and performed a potential energy surface scan of the N–O stretching coordinate. Surprisingly, we found that thermal N–O bond rupture of **AO** led to a rearrangement reaction that included an H-transfer from C to O (**Figure 4C**). The N–O bond PES scan

showed that the dihedral angle (C–O–N–C) decreased from 174 to 90 ° (**Figure S5A**), which led the molecule through a 6-membered transition state during the N–O bond rupture and H transfer from C to O.

Taking into account the findings of experiment and computation, we considered a pericyclic *syn* elimination featuring a 6-membered transition state (**Figure 4A**) as a plausible reaction mechanism. Such an E_i mechanism was reported before for the preparative conversion of aldehydes into nitriles using oximes[53] underscoring our hypothesis. Notably, the E_i pathway yielded products identical to the homolytic scission under mechanochemical conditions.

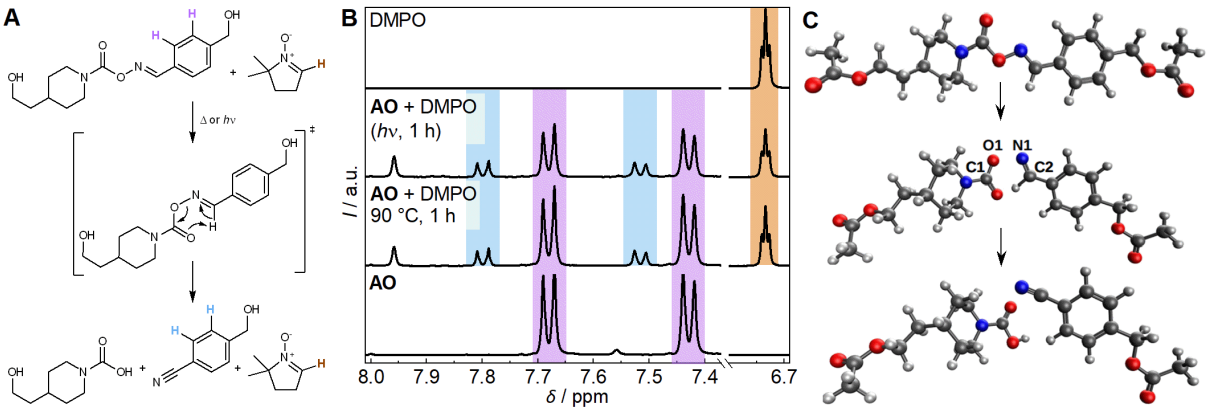

Figure 4. Thermal and photochemical reaction pathways of AO in the presence of DMPO. (A) Reaction scheme including proposed pericyclic *syn* elimination. **(B)** DMPO; irradiated **AO** and DMPO for 1 h; heated **AO** and DMPO for 1 h; and pristine **AO** recorded in DMSO-d_6. **(C)** Computational PES scan indicating rearrangement with H-transfer from C to O at E_a = 139 kJ·mol^{-1} (in DMF).

Since the carbamoylketoximes were thermally stable and only showed non-specific degradation upon heating at 170 °C, we deemed an investigation of the thermal reaction pathway futile and hence proceeded with comparative photochemical experiments. Carbamoylketoximes are prominent photobase generators to uncage latent amines,[49,54] yet require the addition of a triplet sensitizer since the photochemical N–O scission occurs from the T_1 state.[55,56] **MKO** was therefore irradiated at 254 nm for 1 h in the presence of DMPO with and without the addition of the typically used photosensitizer 4-methoxyacetophenone (MAP, **Figure 5A**). While irradiation of **AO** with light in the presence of DMPO yielded the expected nitrile without the consumption of the spin trap (**Figure 4B**), the depletion of DMPO at 6.80 ppm was observed for the irradiation of **MKO** (**Figure 5B**). This underscored the pericyclic character of the aldoxime photoreaction and the homolytic character of the ketoxime

photoreaction. The aromatic protons of **MKO** showed a small shift after trapping and overlapped with two peaks around 7.4 ppm resulting from incomplete trapping in 1 h in the absence of MAP. **MKO** photolysis was greatly accelerated by MAP, emphasizing the scission from the T_1 state (**Figure S8** and **S9**).

Computational multireference simulations supported these experiments. Using the Complete Active Space Self-Consistent Field (CASSCF) approach, we found that the T_1 state was stabilized during N–O bond rupture induced by end-to-end stretching of **MKO** and **TKO** (**Figure S6**). This observation was further underpinned using the Spin-Flip TD-DFT[57] approach to calculate the number of unpaired electrons, which transitioned from zero to two upon bond rupture (**Figure S7**). This finding plausibly explained the thermal stability of the N–O bond in the ketoxime derivatives, since (i) direct access to the reactive T_1 state is spin forbidden and (ii) the E_i mechanism cannot proceed as it involves the transfer of a proton, which is replaced with R = Me or *t*Bu in the ketoximes.

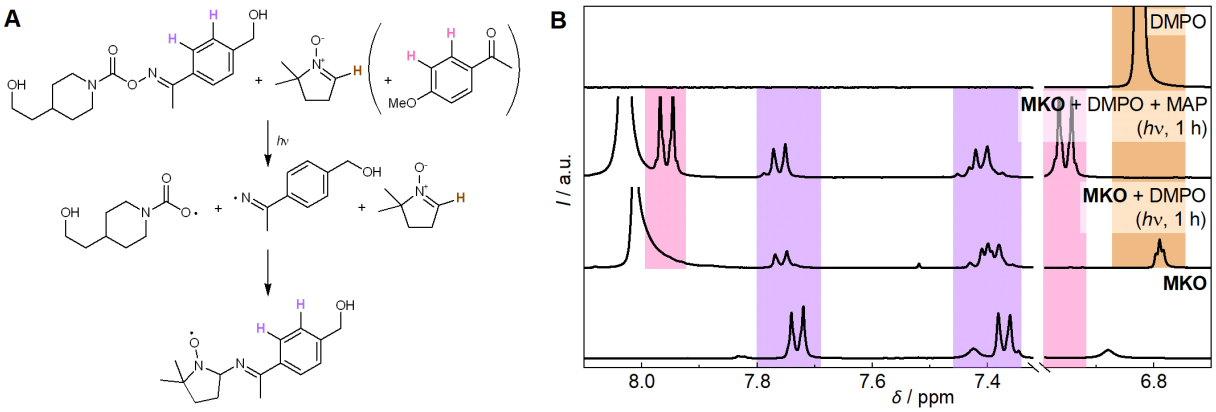

Figure 5. Thermal and photochemical reaction pathways of MKO in the presence of DMPO and MAP. (A) Reaction scheme (focusing exclusively on the NMR-observable potential products). **(B)** DMPO; irradiated **MKO**, DMPO, and MAP for 1 h; irradiated **MKO** and DMPO for 1 h; pristine **MKO** recorded in $CDCl_3$.

Conclusion

We have shown the development of carbamoyloximes as a mechanophore class in which the mechanochemical reaction rates counterintuitively increase alongside the thermal and photochemical stabilities (**Figure 6**). All carbamoyloxime mechanophores undergo homolytic bond scission under mechanochemical conditions and their mechanochemical reaction rates increase with the degree of

substitution on the α-substituent, likely because of the destabilization of the N–O bond and the stabilization of the formed iminyl radical by hyperconjugation.

Surprisingly, the mechanochemical reaction pathway diverges considerably from its thermal and photochemical counterparts. For carbamoylaldoximes, both heat and light induce a pericyclic *syn* elimination, thereby significantly decrease the activation energy, and subsequently render these mechanophores thermally and photochemically labile. For carbamoylketoximes, this pathway is not accessible and homolytic bond scission at the N–O bond dominates, although only from the T_1 state. The inaccessibility of both the E_i mechanism and the spin forbidden T_1 excitation plausibly explain the high thermal and photochemical stability of the carbamoylketoxime mechanophores.

Current approaches to mechanophore discovery are limited by the interconnection of the zero-force and force-modified reaction trajectories, since both are oftentimes identical or entangled. Here we provided an example where the mechanochemical and thermal reaction pathways diverge, hence increasing mechanochemical scission rate and thermal stability at the same time. Such mechanistic considerations may play an important role in the future of systematic mechanophore discovery.

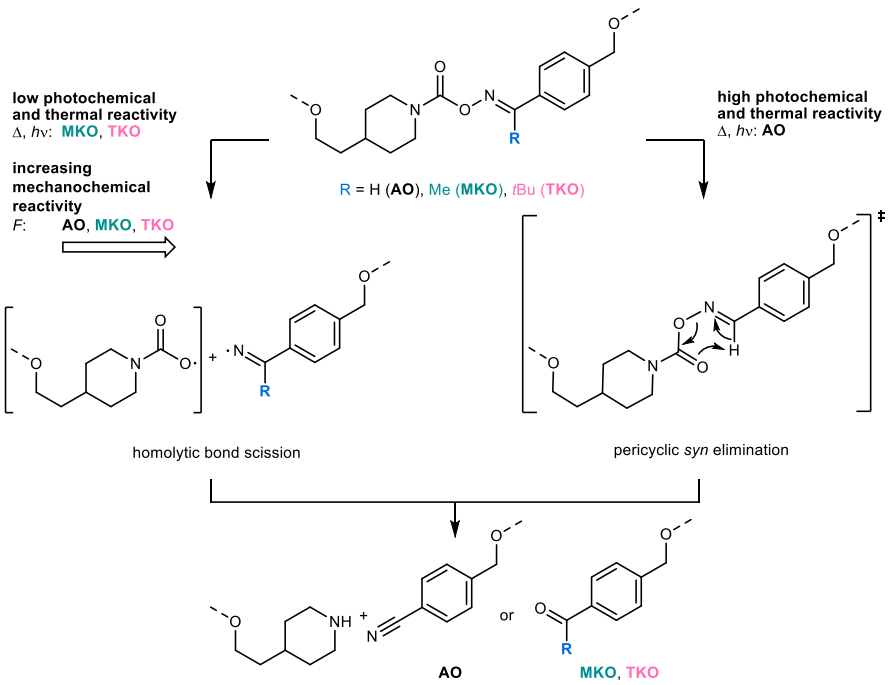

Figure 6. Summarizing scheme of the possible reaction mechanisms of carbamoyloximes. While all carbamoyloximes cleave homolytically under mechanochemical conditions, only the carbamoylaldoximes (**AO**) undergo a pericyclic *syn* elimination under heat and light. Concurrently, carbamoylketoximes (**MKO** and **TKO**) are thermally and photochemically stable while showing increased mechanochemical reaction rates.

Data availability

All data of this study are documented within the manuscript and its Supplemental Information and are publicly available in Zenodo at https://doi.org/10.5281/zenodo.10226890.

Acknowledgements

The authors thank Rainer Haas and Michael Pohl for their extensive support with GPC measurements. Funding is acknowledged from German Research Foundation for 503981124 (R.G.) and 508998124 (R.G., S.S.) as well as from the Federal Ministry of Education and Research for 031B1148A (R.G., S.A.)

Author contributions

Robert Göstl: supervision (lead); project administration (lead); conceptualization (lead); funding acquisition; review and editing (equal). Tim Neudecker: supervision (equal); conceptualization (supporting); funding acquisition; writing – review and editing (equal). Simay Aydonat: writing – original draft preparation (lead); data curation; formal analysis; investigation; validation; visualization, writing – review and editing (equal). Davide Campagna: conceptualization (supporting); data curation; formal analysis; investigation; validation; visualization. Sourabh Kumar: data curation; formal analysis; investigation. Sonja Storch: investigation.

Declaration of interests

The authors declare no competing interests.

References

1. Lenhardt, J.M., Black Ramirez, A.L., Lee, B., Kouznetsova, T.B., and Craig, S.L. (2015). Mechanistic Insights into the Sonochemical Activation of Multimechanophore Cyclopropanated Polybutadiene Polymers. Macromolecules *48*, 6396–6403. https://doi.org/10.1021/acs.macromol.5b01677.

2. De Bo, G. (2020). Polymer Mechanochemistry and the Emergence of the Mechanophore Concept. Macromolecules *53*, 7615–7617. https://doi.org/10.1021/acs.macromol.0c01683.

3. Chen, Y., Mellot, G., Luijk, D. van, Creton, C., and Sijbesma, R.P. (2021). Mechanochemical tools for polymer materials. Chem. Soc. Rev. *50*, 4100–4140. https://doi.org/10.1039/D0CS00940G.

4. Peterson, G.I., and Choi, T.-L. (2021). The influence of polymer architecture in polymer mechanochemistry. Chem. Commun. *57*, 6465–6474. https://doi.org/10.1039/D1CC02501E.

5. Watabe, T., and Otsuka, H. (2024). Enhancing the Reactivity of Mechanically Responsive Units via Macromolecular Design. Macromolecules *57*, 425–433. https://doi.org/10.1021/acs.macromol.3c01280.

6. Davis, D.A., Hamilton, A., Yang, J., Cremar, L.D., Van Gough, D., Potisek, S.L., Ong, M.T., Braun, P.V., Martínez, T.J., White, S.R., et al. (2009). Force-induced activation of covalent bonds in mechanoresponsive polymeric materials. Nature *459*, 68–72. https://doi.org/10.1038/nature07970.

7. Chen, Y., Spiering, A.J.H., Karthikeyan, S., Peters, G.W.M., Meijer, E.W., and Sijbesma, R.P. (2012). Mechanically induced chemiluminescence from polymers incorporating a 1,2-dioxetane unit in the main chain. Nat. Chem. *4*, 559–562. https://doi.org/10.1038/nchem.1358.

8. Ducrot, E., Chen, Y., Bulters, M., Sijbesma, R.P., and Creton, C. (2014). Toughening Elastomers with Sacrificial Bonds and Watching Them Break. Science *344*, 186–189. https://doi.org/10.1126/science.1248494.

9. Wang, Q., Gossweiler, G.R., Craig, S.L., and Zhao, X. (2014). Cephalopod-inspired design of electro-mechano-chemically responsive elastomers for on-demand fluorescent patterning. Nat. Commun. *5*, 4899. https://doi.org/10.1038/ncomms5899.

10. Kato, S., Furukawa, S., Aoki, D., Goseki, R., Oikawa, K., Tsuchiya, K., Shimada, N., Maruyama, A., Numata, K., and Otsuka, H. (2021). Crystallization-induced mechanofluorescence for visualization of polymer crystallization. Nat. Commun. *12*, 126. https://doi.org/10.1038/s41467-020-20366-y.

11. Qian, H., Purwanto, N.S., Ivanoff, D.G., Halmes, A.J., Sottos, N.R., and Moore, J.S. (2021). Fast, reversible mechanochromism of regioisomeric oxazine mechanophores: Developing in situ responsive force probes for polymeric materials. Chem *7*, 1080–1091. https://doi.org/10.1016/j.chempr.2021.02.014.

12. Overholts, A.C., Granados Razo, W., and Robb, M.J. (2023). Mechanically gated formation of donor–acceptor Stenhouse adducts enabling mechanochemical multicolour soft lithography. Nat. Chem. *15*, 332–338. https://doi.org/10.1038/s41557-022-01126-5.

13. Traeger, H., Sagara, Y., Kiebala, D.J., Schrettl, S., and Weder, C. (2021). Folded Perylene Diimide Loops as Mechanoresponsive Motifs. Angew. Chem. Int. Ed. *60*, 16191–16199. https://doi.org/10.1002/anie.202105219.

14. Ramirez, A.L.B., Kean, Z.S., Orlicki, J.A., Champhekar, M., Elsakr, S.M., Krause, W.E., and Craig, S.L. (2013). Mechanochemical strengthening of a synthetic polymer in response to typically destructive shear forces. Nat. Chem. *5*, 757–761. https://doi.org/10.1038/nchem.1720.

15. Diesendruck, C.E., Peterson, G.I., Kulik, H.J., Kaitz, J.A., Mar, B.D., May, P.A., White, S.R., Martínez, T.J., Boydston, A.J., and Moore, J.S. (2014). Mechanically triggered heterolytic unzipping of a low-ceiling-temperature polymer. Nat. Chem. *6*, 623–628. https://doi.org/10.1038/nchem.1938.

16. Wang, J., Kouznetsova, T.B., Boulatov, R., and Craig, S.L. (2016). Mechanical gating of a mechanochemical reaction cascade. Nat. Commun. *7*, 13433. https://doi.org/10.1038/ncomms13433.

17. Chen, Z., Mercer, J.A.M., Zhu, X., Romaniuk, J.A.H., Pfattner, R., Cegelski, L., Martinez, T.J., Burns, N.Z., and Xia, Y. (2017). Mechanochemical unzipping of insulating polyladderene to semiconducting polyacetylene. Science *357*, 475–479. https://doi.org/10.1126/science.aan2797.

18. Lin, Y., Kouznetsova, T.B., Chang, C.-C., and Craig, S.L. (2020). Enhanced polymer mechanical degradation through mechanochemically unveiled lactonization. Nat. Commun. *11*, 4987. https://doi.org/10.1038/s41467-020-18809-7.

19. Nixon, R., and De Bo, G. (2020). Three concomitant C–C dissociation pathways during the mechanical activation of an N-heterocyclic carbene precursor. Nat. Chem. *12*, 826–831. https://doi.org/10.1038/s41557-020-0509-1.

20. Hsu, T.-G., Liu, S., Guan, X., Yoon, S., Zhou, J., Chen, W.-Y., Gaire, S., Seylar, J., Chen, H., Wang, Z., et al. (2023). Mechanochemically accessing a challenging-to-synthesize depolymerizable polymer. Nat. Commun. *14*, 225. https://doi.org/10.1038/s41467-023-35925-2.

21. O'Neill, R.T., and Boulatov, R. (2021). The many flavours of mechanochemistry and its plausible conceptual underpinnings. Nat. Rev. Chem. *5*, 148–167. https://doi.org/10.1038/s41570-020-00249-y.

22. Kauzmann, W., and Eyring, H. (1940). The Viscous Flow of Large Molecules. J. Am. Chem. Soc. *62*, 3113–3125. https://doi.org/10.1021/ja01868a059.

23. Hickenboth, C.R., Moore, J.S., White, S.R., Sottos, N.R., Baudry, J., and Wilson, S.R. (2007). Biasing reaction pathways with mechanical force. Nature *446*, 423–427. https://doi.org/10.1038/nature05681.

24. Dopieralski, P., Ribas-Arino, J., Anjukandi, P., Krupicka, M., Kiss, J., and Marx, D. (2013). The Janus-faced role of external forces in mechanochemical disulfide bond cleavage. Nat. Chem. *5*, 685–691. https://doi.org/10.1038/nchem.1676.

25. Wang, J., Kouznetsova, T.B., Niu, Z., Ong, M.T., Klukovich, H.M., Rheingold, A.L., Martinez, T.J., and Craig, S.L. (2015). Inducing and quantifying forbidden reactivity with single-molecule polymer mechanochemistry. Nat. Chem. *7*, 323–327. https://doi.org/10.1038/nchem.2185.

26. Beedle, A.E.M., Mora, M., Davis, C.T., Snijders, A.P., Stirnemann, G., and Garcia-Manyes, S. (2018). Forcing the reversibility of a mechanochemical reaction. Nat. Commun. *9*, 3155. https://doi.org/10.1038/s41467-018-05115-6.

27. Liu, Y., Holm, S., Meisner, J., Jia, Y., Wu, Q., Woods, T.J., Martinez, T.J., and Moore, J.S. (2021). Flyby reaction trajectories: Chemical dynamics under extrinsic force. Science *373*, 208–212. https://doi.org/10.1126/science.abi7609.

28. Ding, S., Wang, W., Germann, A., Wei, Y., Du, T., Meisner, J., Zhu, R., and Liu, Y. (2024). Bicyclo[2.2.0]hexene: A Multicyclic Mechanophore with Reactivity Diversified by External Forces. J. Am. Chem. Soc. *146*, 6104–6113. https://doi.org/10.1021/jacs.3c13589.

29. Horst, M., Meisner, J., Yang, J., Kouznetsova, T.B., Craig, S.L., Martínez, T.J., and Xia, Y. (2024). Mechanochemistry of Pterodactylane. J. Am. Chem. Soc. *146*, 884–891. https://doi.org/10.1021/jacs.3c11293.

30. Sun, Y., Neary, W.J., Burke, Z.P., Qian, H., Zhu, L., and Moore, J.S. (2022). Mechanically Triggered Carbon Monoxide Release with Turn-On Aggregation-Induced Emission. J. Am. Chem. Soc. *144*, 1125–1129. https://doi.org/10.1021/jacs.1c12108.

31. Jung, S., and Yoon, H.J. (2021). Mechanical Force for the Transformation of Aziridine into Imine. Angew. Chem. Int. Ed. *60*, 23564–23568. https://doi.org/10.1002/anie.202109358.

32. Klok, H.-A., Herrmann, A., and Göstl, R. (2022). Force ahead: Emerging Applications and Opportunities of Polymer Mechanochemistry. ACS Polym. Au *2*, 208–212. https://doi.org/10.1021/acspolymersau.2c00029.

33. Willis-Fox, N., Watchorn-Rokutan, E., Rognin, E., and Daly, R. (2023). Technology pull: scale-up of polymeric mechanochemical force sensors. Trends Chem. *5*, 415–431. https://doi.org/10.1016/j.trechm.2023.02.005.

34. Sakai, H., Sumi, T., Aoki, D., Goseki, R., and Otsuka, H. (2018). Thermally Stable Radical-Type Mechanochromic Polymers Based on Difluorenylsuccinonitrile. ACS Macro Lett. *7*, 1359–1363. https://doi.org/10.1021/acsmacrolett.8b00755.

35. Campagna, D., and Göstl, R. (2022). Mechanoresponsive Carbamoyloximes for the Activation of Secondary Amines in Polymers. Angew. Chem. Int. Ed. *61*, e202207557. https://doi.org/10.1002/anie.202207557.

36. Pratt, D.A., Blake, J.A., Mulder, P., Walton, J.C., Korth, H.-G., and Ingold, K.U. (2004). O−H Bond Dissociation Enthalpies in Oximes: Order Restored. J. Am. Chem. Soc. *126*, 10667–10675. https://doi.org/10.1021/ja047566y.

37. Kohn, W., and Sham, L.J. (1965). Self-Consistent Equations Including Exchange and Correlation Effects. Phys. Rev. *140*, A1133–A1138. https://doi.org/10.1103/PhysRev.140.A1133.

38. Hohenberg, P., and Kohn, W. (1964). Inhomogeneous Electron Gas. Phys. Rev. *136*, B864–B871. https://doi.org/10.1103/PhysRev.136.B864.

39. Beyer, M.K. (2000). The mechanical strength of a covalent bond calculated by density functional theory. J. Chem. Phys. *112*, 7307–7312. https://doi.org/10.1063/1.481330.

40. Nikitina, E.A., Khavryutchenko, V.D., Sheka, E.F., Barthel, H., and Weis, J. (1999). Deformation of Poly(dimethylsiloxane) Oligomers under Uniaxial Tension: Quantum Chemical View. J. Phys. Chem. A *103*, 11355–11365. https://doi.org/10.1021/jp990221v.

41. Becke, A.D. (1988). Density-functional exchange-energy approximation with correct asymptotic behavior. Phys. Rev. A *38*, 3098–3100. https://doi.org/10.1103/PhysRevA.38.3098.

42. Lee, C., Yang, W., and Parr, R.G. (1988). Development of the Colle-Salvetti correlation-energy formula into a functional of the electron density. Phys. Rev. B *37*, 785–789. https://doi.org/10.1103/PhysRevB.37.785.

43. Becke, A.D. (1993). A new mixing of Hartree–Fock and local density-functional theories. J. Chem. Phys. *98*, 1372–1377. https://doi.org/10.1063/1.464304.

44. Hehre, W.J., Ditchfield, R., and Pople, J.A. (2003). Self—Consistent Molecular Orbital Methods. XII. Further Extensions of Gaussian—Type Basis Sets for Use in Molecular Orbital Studies of Organic Molecules. J. Chem. Phys. *56*, 2257–2261. https://doi.org/10.1063/1.1677527.

45. Klein, I.M., Husic, C.C., Kovács, D.P., Choquette, N.J., and Robb, M.J. (2020). Validation of the CoGEF Method as a Predictive Tool for Polymer Mechanochemistry. J. Am. Chem. Soc. *142*, 16364–16381. https://doi.org/10.1021/jacs.0c06868.

46. Cravotto, G., Gaudino, E.C., and Cintas, P. (2013). On the mechanochemical activation by ultrasound. Chem. Soc. Rev. *42*, 7521–7534. https://doi.org/10.1039/C2CS35456J.

47. McFadden, M.E., Overholts, A.C., Osler, S.K., and Robb, M.J. (2023). Validation of an Accurate and Expedient Initial Rates Method for Characterizing Mechanophore Reactivity. ACS Macro Lett. *12*, 440–445. https://doi.org/10.1021/acsmacrolett.3c00054.

48. Overholts, A.C., McFadden, M.E., and Robb, M.J. (2022). Quantifying Activation Rates of Scissile Mechanophores and the Influence of Dispersity. Macromolecules *55*, 276–283. https://doi.org/10.1021/acs.macromol.1c02232.

49. Kanji, S., Satoshi, N., and Masamitsu, S. (2005). Thermally Stable Carbamates as Novel Photobase Generator. J. Photopolym. Sci. Technol. *18*, 141–148. https://doi.org/10.2494/photopolymer.18.141.

50. Wang, Y., Guan, Q., Guo, Y., Sun, L., Neisiany, R.E., Guo, X., Huang, H., Yang, L., and You, Z. (2024). Bone-inspired stress-gaining elastomer enabled by dynamic molecular locking. Sci. Adv. *10*, eadk5177. https://doi.org/10.1126/sciadv.adk5177.

51. Liu, W.-X., Zhang, C., Zhang, H., Zhao, N., Yu, Z.-X., and Xu, J. (2017). Oxime-Based and Catalyst-Free Dynamic Covalent Polyurethanes. J. Am. Chem. Soc. *139*, 8678–8684. https://doi.org/10.1021/jacs.7b03967.

52. Kemp, T.J. (1999). Kinetic Aspects of Spin Trapping. Prog. React. Kinet. Mech. *24*, 287–358. https://doi.org/10.3184/007967499103165102.

53. Laulhé, S., Gori, S.S., and Nantz, M.H. (2012). A Chemoselective, One-Pot Transformation of Aldehydes to Nitriles. J. Org. Chem. *77*, 9334–9337. https://doi.org/10.1021/jo301133y.

54. Hwang, H., Jang, D.-J., and Chae, K.H. (1999). Photolysis reaction mechanism of dibenzophenoneoxime hexamethylenediurethane, a new type of photobase generator. J. Photochem. Photobiol. Chem. *126*, 37–42. https://doi.org/10.1016/S1010-6030(99)00129-X.

55. Lalevée, J., Allonas, X., Fouassier, J.P., Tachi, H., Izumitani, A., Shirai, M., and Tsunooka, M. (2002). Investigation of the photochemical properties of an important class of photobase generators: the O-acyloximes. J. Photochem. Photobiol. Chem. *151*, 27–37. https://doi.org/10.1016/S1010-6030(02)00174-0.

56. McBurney, R.T., and Walton, J.C. (2013). Dissociation or Cyclization: Options for a Triad of Radicals Released from Oxime Carbamates. J. Am. Chem. Soc. *135*, 7349–7354. https://doi.org/10.1021/ja402833w.

57. Shao, Y., Head-Gordon, M., and Krylov, A.I. (2003). The spin–flip approach within time-dependent density functional theory: Theory and applications to diradicals. J. Chem. Phys. *118*, 4807–4818. https://doi.org/10.1063/1.1545679.